

pubs.acs.org/Macromolecules Article

Dynamic Mechanical Properties of Self-Assembled Bottlebrush Polymer Networks

Shifeng Nian and Li-Heng Cai*



Cite This: Macromolecules 2022, 55, 8058-8066



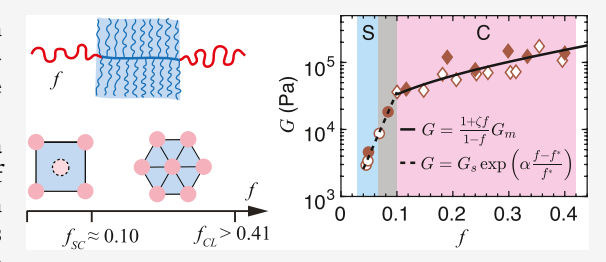
ACCESS I

III Metrics & More

Article Recommendations

Supporting Information

ABSTRACT: We systematically investigate the effects of composition on the dynamic mechanical properties of bottlebrush polymer networks self-assembled by linear—bottlebrush—linear triblock copolymers. We fix the molecular architecture of the bottlebrush, which consists of 51 poly(dimethyl siloxane) (PDMS) side chains of 5 kg/mol and has a molecular weight of 255 kg/mol, and increase only the volume fraction f of the linear poly(benzyl methacrylate) (PBnMA) blocks. As f increases from 0.05 to 0.41, the network shear modulus G at room temperature increases from \sim 4 to \sim 100 kPa. Yet, depending on the network morphology, the



relation between G and f exhibits two regimes. (i) For sphere morphology, G is nearly a constant; yet, because of a large fraction of loops, the absolute value of G is about 40% of the stiffness G_m of the PDMS bottlebrush matrix. (ii) For cylinder morphology, G increases slowly with f but remains nearly 4 orders of magnitude lower than 10^9 Pa for the glassy cylinders formed by the end PBnMA blocks. We explain this remarkable behavior by modeling the polymer as a polycrystalline material consisting of randomly oriented grains, and each grain is a fiber-reinforced composite. We propose a modified Halpin—Tsai model to describe the shear modulus of such a polycrystalline material: $G = G_m(1+\zeta f)/(1-f)$, in which ζ is an adjustable parameter that describes the grain size relative to the fiber diameter. Above the glass-transition temperature of end blocks, the reinforcement to network modulus from the glassy fibers diminishes, such that G becomes a constant of the matrix stiffness. Our results not only reveal previously unexplored molecule—structure—property relations of self-assembled bottlebrush polymer networks but also provide a new class of soft, solvent-free, and reprocessable polymeric materials with a wide range of controllable stiffness.

1. INTRODUCTION

A bottlebrush polymer consists of a long linear backbone densely grafted by many linear side chains. Reminiscent of the difference between spaghetti and sausage, a bottlebrush polymer is effectively a "fat" linear polymer but with an entanglement molecular weight (MW) much higher than that of its flexible linear counterparts. 1,2 Thus, networks formed by cross-linking bottlebrush polymers are often free of entanglements. Because the stiffness of an unentangled polymer network is inversely proportional to the MW of a network strand and the MW of bottlebrush molecules can be very large, bottlebrush polymer networks (BPNs) are often extremely soft. 1-6 Indeed, besides the most commonly seen hydrogels, 7-9 BPNs are probably the only class of synthetic soft materials that can have stiffness in the range of 10-10⁵ Pa, matching that of most "watery" biological tissues and cells. 10 Unlike hydrogels, which contain a large amount of water that can leach out to deteriorate materials properties, BPNs are "dry" and contain no water or solvents whatsoever. Moreover, the extreme softness allows BPNs to be easily deformed to a large extent under small mechanical stress. The exceptional combination of softness and deformability enables the application of BPNs as ultrasensitive sensors, 11 dielectric elastomer actuators, 12 stretchable electronics, 13 and substrate materials for studying cell mechanics. Consequently, bottlebrush polymer networks emerge as a new class of soft materials of both fundamental and technological importance.

Depending on the network topology, BPNs can be either randomly or end cross-linked. In a random network, precursor bottlebrush polymers are cross-linked among functional groups on the bottlebrush backbone 1,14,15 or side chains 16,17 through permanent 18,19 or dynamic covalent bonds. 20,21 This cross-linking process, however, randomly divides a bottlebrush into sections with a wide distribution in MW. Under large deformations, the stress is localized and amplified along relatively short bottlebrush sections to result in network fracture. As a result, the randomly cross-linked BPNs are often brittle. By contrast, in an end cross-linked BPN, each network strand is prescribed to be the whole bottlebrush polymer; this offers better control over mechanical properties under large deformations. Moreover, end cross-linked BPNs can be formed by a one-step self-assembly process rather than additional

Received: June 10, 2022 Revised: August 5, 2022 Published: September 7, 2022





chemical cross-linking. For example, linear—bottlebrush—linear (LBBL) triblock copolymers consisting of an incompatible, soft elastomeric bottlebrush and two hard, glassy linear blocks microphase separate to a network structure. In such a network, the cross-linkers are hard domains formed by the glassy end blocks, whereas the soft network strands are the elastomeric bottlebrush polymers. Above the melting point of the end blocks or in the presence of solvents, the glassy domains can dissociate to transform the network from a solid to a liquid. Such a stimulus-triggered solid-to-liquid transition enables the physically cross-linked BPNs as inks for direct-write 3D printing. Yet, the effects of composition on the properties of self-assembled bottlebrush polymer networks remain to be elucidated.

Recently, we studied the self-assembly of strongly segregated LBBL triblock polymers (Figure 1).²² In an LBBL polymer, the

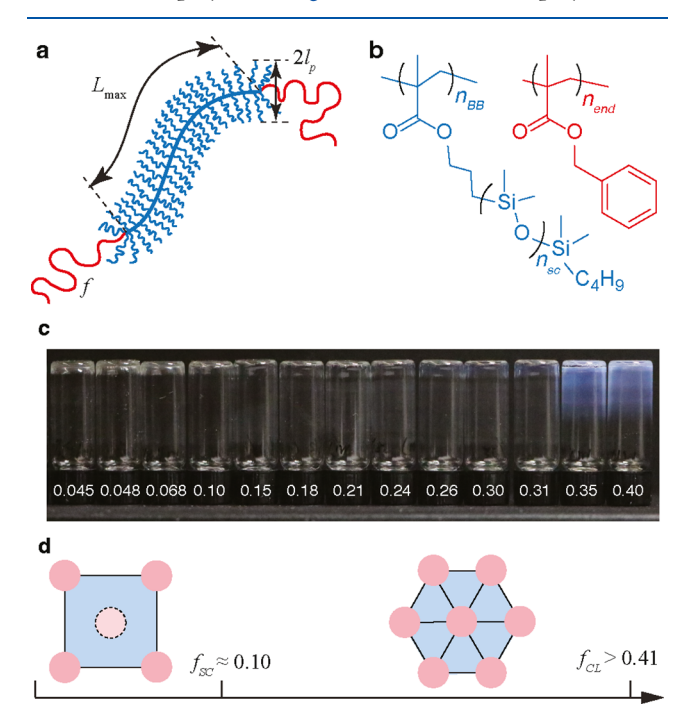


Figure 1. Molecular design and microstructure of self-assembled bottlebrush polymer networks. (a) Schematic of a linear-bottlebrush-linear (LBBL) triblock copolymer. F is the volume fraction of end linear blocks. The flexibility of a bottlebrush polymer is defined as $\kappa \equiv L_{\rm max}/2l_{\rm p}$, in which $l_{\rm p}$ and $L_{\rm max}$ are, respectively, the persistence length and the contour length of the bottlebrush; for a semiflexible bottlebrush, $\kappa \approx 1$. (b) In our system, the side chain of the middle bottlebrush block is a linear polydimethylsiloxane (PDMS) with a molecular weight of 5000 g/mol, whereas the end blocks are linear poly(benzyl methacrylate) (PBnMA). We fix the number of side chains per bottlebrush at $n_{\rm BB} = 51$ while changing the number of repeating units $n_{\rm L}$ of the end linear blocks from 30 to 570. This results in triblock copolymers that have the same semiflexible bottlebrush middle block of contour length $L_{\rm max}$ = 12.8 nm and persistence length $l_p = 5.8$ nm, whereas the volume fraction f of end blocks varies from 0.045 to 0.40. (c) Self-assembled polymers are optically transparent at f < 0.26 but gradually become blue at $f \ge 0.26$, and the blue color becomes brighter and more obvious at $f \ge 0.36$. (d) Cross-over volume fraction between sphere and cylinder morphology is in the range of 0.07-0.10. The self-assembled microstructure remains to be a hexagonal cylinder up to the fraction of 0.41.²² Light red: domains formed by end blocks; light blue: soft bottlebrush PDMS matrix. Reproduced with permission from Macromolecules 54, 9361-9371 (2021). Copyright 2021 American Chemical Society.

two end linear blocks are poly(benzyl methacrylate) (PBnMA), whereas the middle block is a bottlebrush formed by polymerizing 51 methyl acrylate-terminated polydimethylsiloxane (MA-PDMS) with a molecular weight (MW) of 5000 g/mol. The polydispersity index of the bottlebrush is relatively narrow of 1.15. Using the bottlebrush PDMS (bbPDMS) as a macroinitiator, we synthesize a series of PBnMA-bbPDMS-PBnMA triblock copolymers with the volume fraction *f* of the end blocks ranging from 0.045 to 0.41 (Table 1 and Supporting Information).²² Importantly, all triblock copolymers have the same middle block, which is a semiflexible bottlebrush with the backbone contour length $L_{\rm max} \approx 13~{\rm nm}$ about twice that of the persistence length. We found that the bottlebrush can rearrange its constituent linear side chains to form domains remarkably larger than the contour length of the bottlebrush backbone. Moreover, the semiflexible bottlebrush dramatically widens the regime for hexagonal cylinder morphology that is associated with $f \in (0.10, >0.41)$, which is wider than that for flexible linear block copolymers with $f \in$ (0.14, 0.35) and that predicted by recent self-consistent field theory for linear-bottlebrush block copolymers of the same chemistry and molecular architecture.

Here, we systematically investigate the effects of composition on the dynamic mechanical properties of BPNs selfassembled by LBBL triblock copolymers. As f increases from 0.05 to 0.41, the network shear modulus G at room temperature increases from ~4 to ~100 kPa. Yet, depending on the network morphology, the relation between G and f exhibits two regimes. At small f or sphere morphology, G is nearly a constant; yet, because of a large fraction of loops, the absolute value of G is about 40% of that predicted for the soft bottlebrush matrix. At relatively high *f* or cylinder morphology, G increases slowly with f but remains nearly 4 orders of magnitude lower than that of hard glassy cylinders. By modeling the polymers as a fiber-reinforced composite, we develop a modified Halpin-Tsai model that can well describe the network shear modulus of cylinder morphology. At temperatures well above the glass-transition temperature $T_{\rm g}$ of the end blocks, the reinforcement to the network modulus from the glassy fibers diminishes, such that the shear modulus becomes a constant of the matrix stiffness. Our results not only help establish the molecule-structure-property relation of self-assembled BPNs but also provide a new class of soft, solvent-free, and reprocessable polymeric materials with a wide range of controllable stiffness.

2. RESULTS AND DISCUSSION

We use a stress-controlled rheometer to quantify the dynamic mechanical properties of the BPNs (see Experimental Section). Yet, for strongly segregated block copolymers like our systems, their self-assembly can be easily trapped in metastable states to result in uncontrollable macroscopic mechanical properties. Therefore, it is critical to determine the annealing conditions for achieving an equilibrium microstructure. To this end, we choose the polymer with f = 0.40 (sample S_{13} in Table 1) as an example to determine the annealing conditions. This polymer has the highest volume fraction among all the polymers explored in this study. Therefore, the polymer has the highest segregation strength and is the most difficult to reach the equilibrium state.

We explore combinations of solvent and thermal annealing to equilibrate the polymer. We use the same solvent casting method to prepare polymer films for in situ rheological

Table 1. Molecular Parameters of Self-Assembled Bottlebrush Polymer Networks^a

		mid	ldle block		triblock			mechanical properties		
batch	sample	M _{sc} (kDa)	n_{BB}	PDI	n_{end}	f	PDI	G (kPa) @ 20 °C	G (kPa) @ 180 °C	γ _s (%)
1	S_1	5	51	1.15	41	0.045	1.17	2.9	0.067	186
	S_2				44	0.048	1.17	3.4	0.061	160
	S_3				64	0.068	1.18	8.7	0.45	101
	S_4				97	0.10	1.20	36.2	5.1	18.6
	S_5				151	0.15	1.31	38.2	8.6	11.7
	S_6				193	0.18	1.36	66.5	9.2	7.4
	S_7				226	0.21	1.54	55.2	7.9	10.1
	S_8				278	0.24	1.55	67.3	11.4	15.9
	S_9				310	0.26	1.57	70.2	10.1	15.9
	S_{10}				378	0.30	1.60	71.0	15.7	6.32
	S_{11}				396	0.31	1.64	72.6	12.6	10
	S_{12}				478	0.35	1.71	174	15.4	6.33
	S_{13}				570	0.40	1.71	107	11.1	7.3
2	S_{14}			1.18	80	0.084	1.38	19.5	3.1	71.1
	S_{15}				371	0.30	1.57	148	20.6	12.6
3	S_{16}			1.20	275	0.24	1.60	77.9	14.2	15.9
4	S_{17}			1.17	48	0.052	1.20	4.6	0.037	160
	S_{18}				124	0.12	1.26	39.8	5.7	63.5
	S_{19}				436	0.33	1.54	123	8.7	6.3
5	S_{20}			1.17	204	0.19	1.36	120	14.0	15.9
	S_{21}				581	0.40	1.52	138	11.9	5

 $^{{}^{}a}M_{sc}$ molecular weight of side chains; n_{BB} , number of side chains per bottlebrush; n_{end} , number of chemical repeating units for each end linear PBnMA block; f, volume fraction of the end blocks; PDI, polydispersity index; G, shear modulus; and γ_{s} , shear yield strain.

measurements. We dissolve the polymer in toluene at a concentration of 100 mg/mL, pipette about 0.5 mL of solution onto the bottom plate of the rheometer, and cover the solution with a glass cap. Unlike other organic solvents such as chloroform with a vapor pressure of 200 mm Hg at room temperature, toluene is much less volatile with a vapor pressure of 20 mm Hg. This method allows the solvent to slowly evaporate over 10 h, leaving a homogeneous film on the bottom plate. The plate is heated up to 60 °C for an additional 20 min to remove any residual solvent. This method allows preparing a film with a uniform thickness of 60 μ m without air bubbles. Then, we lower the upper plate and trim the excess sample at the edge of the geometry to start thermal annealing of the polymer.

We identify two parameters critical to thermal annealing: (i) waiting time at each temperature point and (ii) the temperate ramping rate for the heating/cooling cycle. The equilibrium annealing conditions are determined if the shear moduli of the polymer upon heating agree with those upon cooling. To do so, for the solvent-annealed polymer, we increase the temperature from 60 to 180 °C at the rate of 2.5 °C/min and hold it at 180 °C for 5 min. Then, we measure the storage (G') and loss (G'') moduli upon cooling/heating between -20and 180 °C. We fix the temperature ramping rate at 0.5 °C/s and vary the waiting time at each temperature point. As the waiting time increases from 1 min to 20 min, the shear moduli upon cooling/heating become closer (Figure 2a-c); this suggests that a longer waiting time promotes equilibrium selfassembly. However, the measurements upon cooling/heating do not overlap. This hysteresis in shear moduli upon cooling/ heating cycle suggests that the waiting time alone is insufficient to anneal the polymer.

Yet, at the longest waiting time of 20 min, the hysteresis is negligible at relatively high temperatures and only becomes pronounced at temperatures lower than 100 °C (Figure 2c).

This behavior suggests that at a relatively low temperature, when the polymer dynamics slow down, the ramping rate might be too fast for the polymers to relax. Therefore, we lower the temperature ramping rate to 1 °C/min and monitor the dependence of shear moduli on waiting time. Specifically, for a solvent-annealed polymer, we increase the temperature from 60 to 180 °C and hold it at 180 °C for 30 min. Upon cooling, at each temperature point, we monitor the shear moduli for 30 min. Both G' and G'' reach stable values after 20 min(Figure S1), indicating that 20 min is sufficient to equilibrate the polymer. Moreover, we use an excess amount of 30 min waiting time throughout all measurements to ensure all polymers are equilibrated. Indeed, the shear moduli for heating and cooling almost overlap, as shown in Figure 2d. A slight difference in storage modulus is observed near the glasstransition temperature $T_{\rm g}$ = 54 °C of PBnMA. This is likely because, near T_g , the mobility of polymer chains changes dramatically; this results in incomplete relaxation of polymers within a finite waiting time, such that the dynamics of polymers exhibit hysteresis upon a cooling/heating cycle. ^{24,25} Nevertheless, these measurements successfully establish an annealing procedure that enables nearly equilibrated polymers at various temperatures.

We use the above procedure to anneal all polymers and explore the effects of composition on dynamic mechanical properties. We focus on stiffness and extensibility, two of the most important mechanical properties of polymer networks. At room temperature, all the networks exhibit a nearly frequency-independent shear storage modulus G', as shown by solid symbols in Figure 3a. Therefore, we take the value of G' at the lowest oscillatory shear frequency, 0.1 rad/s, as the equilibrium shear modulus G. As f increases from 0.048 to 0.40, the shear modulus increases dramatically by nearly 30 times, from 3.4 to 107 kPa, as, respectively, shown by solid blue and red symbols in Figure 3a. This trend is observed from triblock polymers

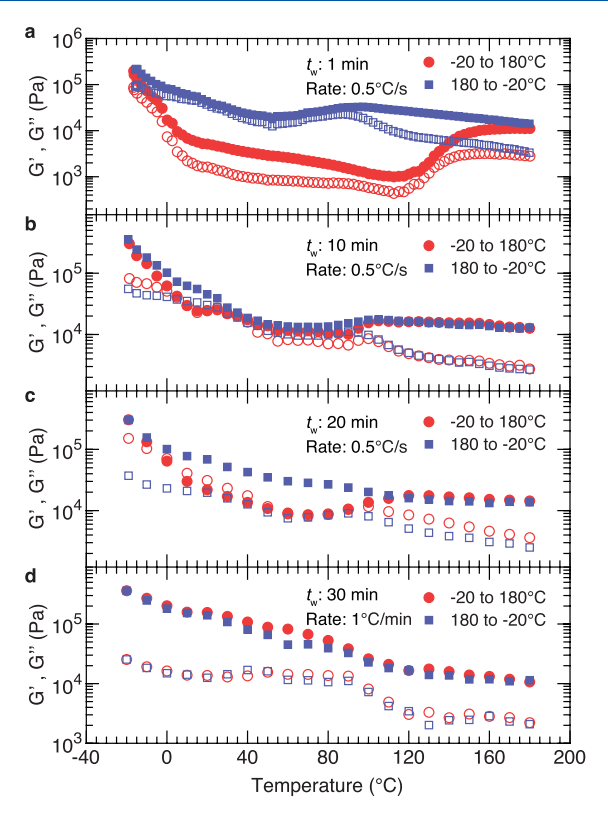


Figure 2. Annealing of bottlebrush polymer networks. We monitor the storage (G', filled symbols) and loss (G'', empty symbols) moduli of the sample with f = 0.40 upon heating/cooling between -20 and $180\,^{\circ}\text{C}$ at various ramping rates and waiting times. (a) Each data point is collected with an interval of 2.5 $^{\circ}\text{C}$ at a ramping rate of 0.5 $^{\circ}\text{C}/\text{s}$. After reaching a temperature, we wait for 1 min before collecting the data. (b) Interval: $5\,^{\circ}\text{C}$; ramping rate: $0.5\,^{\circ}\text{C}/\text{s}$; and waiting time: $10\,^{\circ}\text{min}$. (c) Interval: $10\,^{\circ}\text{C}$; ramping rate: $0.5\,^{\circ}\text{C}/\text{s}$; and waiting time: $20\,^{\circ}\text{min}$. (d) Interval: $10\,^{\circ}\text{C}$; ramping rate: $1\,^{\circ}\text{C}/\text{min}$; and waiting time: $30\,^{\circ}\text{min}$. All measurements are performed at $1\,^{\circ}\text{rad/s}$ and $0.5\%\,^{\circ}$ strain.

synthesized from multiple batches of bottlebrush polymers with the same average number of side chains but slightly different dispersity (filled symbols in Figure S2, and Table 1). These results show that the shear modulus of self-assembled BNPs can be tuned in a wide range by changing the polymer composition only.

In parallel, we use large amplitude oscillatory shear measurements (LAOS) to quantify the extensibility of the self-assembled polymers (Figure 3b). As established in a recent study, 15 in addition to the elongation at break measured by tensile tests, the extensibility of a polymer network can be described by shear yield strain γ_s , above which the storage modulus becomes smaller than the loss modulus, as noted by the arrows in Figure 3b. As f increases from 0.045 to 0.40, γ_s decreases from 1.61 to 0.07 (arrows in Figure 3b). A similar trend is observed for networks based on bottlebrush polymers from different batches (Figure S3). These results show that network extensibility is negatively correlated to stiffness (Figure S4). This behavior is consistent with the classical understanding of polymer networks: stiffer networks are less stretchable. However, at low f < 0.07, γ_s is relatively large at ~100% (Regime I, Figure 3d). This value is much larger than the extensibility expected for a semiflexible bottlebrush, γ_s = $L_{\rm max}/R-1\approx 0$, whose backbone contour length $L_{\rm max}$ is comparable to the mean-square end-to-end distance R of the

backbone. Such a remarkably large extensibility of self-assembled BPNs is likely attributed to the linear end blocks, which can be pulled out from the glassy domains upon large deformations. At large f, however, the glassy domains may become too strong for the end blocks to be pulled out. Consistent with this understanding, at f > 0.10, the self-assembled BNPs exhibit a very small shear yield strain of $\sim 10\%$ (Regime II, Figure 3d).

To further understand the effects of composition on mechanical properties, we explore the composition-microstructure-property relation of the self-assembled BPNs. As expected, the shear modulus G is strongly correlated to the types of microstructures. Yet, the dependence of G on f exhibits two regimes associated with network morphology. In regime I (0.04 < f < 0.07), where the polymers form sphere morphology, G is extremely low at nearly a constant of \sim 4 kPa (blue region, Figure 3c). The constant shear modulus is expected as the polymers form an unentangled polymer network in which the PBnMA spheres act as cross-links, whereas the bottlebrush PDMS molecules act as network strands. In addition, the shear modulus of an unentangled polymer is determined by the MW of the network strand, which is the same for the triblock copolymers. However, the absolute value of ~4 kPa is about 40% of the theoretical prediction for an unentangled polymer network:

$$G \approx \frac{k_{\rm B}T\rho}{M_{\rm bb}} = 9.4 \text{ kPa} \tag{1}$$

where $k_{\rm B}$ is the Boltzmann constant, $T=293~{\rm K}$ is the absolute temperature, $M_{\rm bb}=255~{\rm kg/mol}$ is the mass of PDMS bottlebrush, and $\rho\approx 1~{\rm g/cm^3}$ is the density of PDMS. This difference suggests that only about 40% of the bottlebrush blocks form elastically effective bridges, whereas the rest form elastically ineffective loops, as illustrated in Figure 4a(i). However, the fraction of bridges is significantly lower than ~80% for sphere microstructures self-assembled by conventional linear triblock copolymers. ²⁶

The surprisingly high fraction of loops formed by LBBL triblock polymers is likely attributed to the molecular architecture of the semiflexible bottlebrush. For an ABA triblock copolymer, the probability of forming a loop is proportional to the concentration of A blocks, which is inversely proportional to the volume pervaded by the middle B block. Because all side chains are grafted to a backbone, the size of the semiflexible bottlebrush, 22 $R_{\rm SFB} \approx 13$ nm, is much smaller than that of the flexible linear counterpart of the same MW, $R_{\rm FL} \approx b N^{1/2} \approx 34$ nm, in which b = 1.3 nm is the size of a PDMS Kuhn monomer and N = 670 is the number of Kuhn monomers for a linear PDMS of 255 kDa. For an LBBL triblock copolymer, therefore, the probability for the two end linear blocks to meet to form loops is much higher than that for conventional linear triblock copolymers. Moreover, previous studies showed that, for LBBL polymers, the diameter of a spherical domain, ~10 nm, is comparable to the size of the bottlebrush.²² As a result, the semiflexible bottlebrush does not have to bend to have the two end linear blocks connected to the same spherical domain. This process can avoid the entropic penalty associated with constraining polymer configuration, which is often seen in the loop formation for conventional linear triblock copolymers, where the middle block must change from a linear to a ring-like configuration, as illustrated in Figure 4a(ii). Consequently, for the sphere microstructures

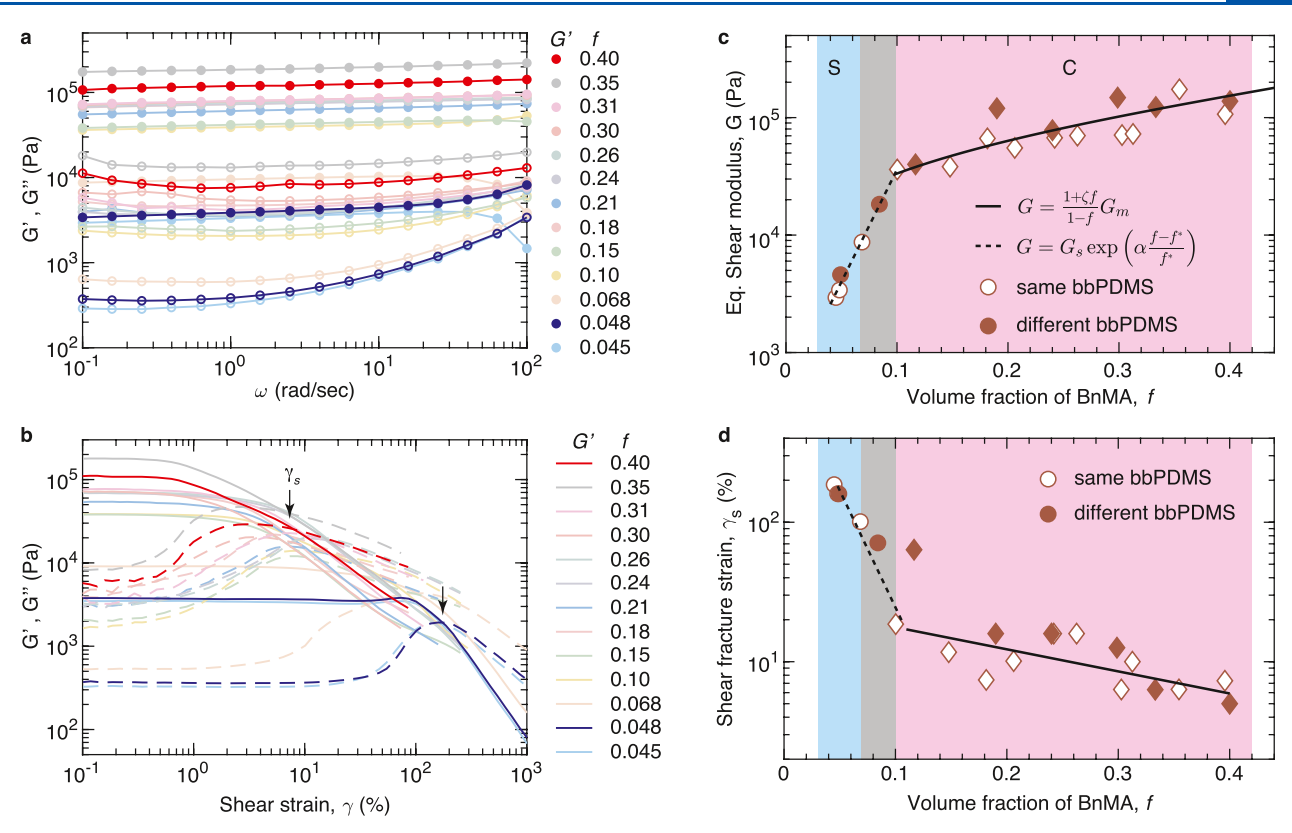


Figure 3. Dynamic mechanical properties of bottlebrush polymer networks. (a) Frequency sweep of polymers with the same bottlebrush middle block (batch 1, Table 1) at 20 °C. Filled symbols: storage modulus G'; empty symbols: loss modulus G''. (b) Large amplitude oscillatory shear (LAOS) measurements of polymers with the same bottlebrush middle block (batch 1, Table 1) at 20 °C. Solid lines: G'; dashed lines, G''. (c) Dependence of equilibrium shear modulus on the volume fraction of end blocks. The dashed line is the best fit to data for the small window 0.07 < f < 0.10, in which the polymers transition from sphere to cylinder morphology: $G = G_s \exp[\alpha(f - f^*)/f^*]$, in which $G_s = 4$ kPa is the shear modulus for sphere morphology, $f^* = 0.05$, and $\alpha = 2.2$. The solid line is the best fit to data for polymers with cylinder morphology using a modified Halpin–Tsai model for a polycrystalline fiber-reinforced composite [eq 3]: $G = G_m(1 + \zeta f)/(1 - f)$, in which $G_m = 9.4$ kPa is the shear modulus of the soft bottlebrush PDMS matrix [eq 1], and the fitting parameter $\zeta = 22$ describes the effective aspect ratio of PBnMA cylinders. (d) Dependence of shear yield strain on the volume fraction of end blocks. Lines are guidance for the eye. For f < 0.10, the shear yield strain scales with shear modulus by a power of -1/2, $\gamma_s \sim G^{-1/2}$; for f > 0.10, γ_s suddenly drops to $\sim 10\%$ (Figure S4). Empty and solid symbols are triblock copolymers with the same and different batches of middle blocks, respectively. Light blue region: sphere morphology (S); gray region: cross-over from sphere to cylinder morphology; and light red region: cylinder morphology (C).

self-assembled by LBBL polymers, the fraction of loops is nearly the same as that of the bridges. Nevertheless, the network stiffness is largely determined by the bottlebrush molecular weight.

As the polymer morphology transitions from sphere to cylinder (0.07 < f < 0.10), G increases by nearly 10 times from ~4 to ~40 kPa (gray region, Figure 3c). Moreover, such an increase can be described by an exponential form (dashed line, Figure 3c), highlighting a strong influence of network morphology on stiffness. Interestingly, as the polymers form cylinder morphology (regime II, 0.10 < f < 0.41), G increases slowly with f and becomes somewhat saturated around 100 kPa at high-volume fractions (symbols in the light red region in Figure 3c). This value is about half of the entanglement modulus, 200 kPa, of linear PDMS.²⁷ Such a low shear modulus is in striking contrast to that seen for conventional thermoplastic elastomers self-assembled by linear triblock copolymers such as poly(styrene-b-butadiene-b-styrene) (SBS)^{28,29} or poly(styrene-*b*-isoprene-*b*-styrene) (SIS).³⁰ For instance, at f > 0.34, these linear triblock copolymers form a lamellar morphology, in which the soft domains are sandwiched between the stiff planes. Although the shear modulus of an oriented lamellar stack depends on the direction

of shear deformation, on average it is largely determined by that of the hard glassy planes and is typically above 100 MPa. Even at 0.18 < f < 0.34, in which the linear triblock copolymers form cylinder morphology, ³¹ the network shear modulus remains about 5 MPa, ³² nearly 50 times stiffer than LBBL polymers of the same morphology. These results highlight the unique mechanical behavior of LBBL polymers with cylinder morphology.

To explain the remarkable stiffness of LBBL polymers with cylinder morphology, we consider the polymers as a polycrystalline material consisting of grains randomly oriented in space, as illustrated in Figure 4b(i). Within each grain, PBnMA is dispersed as a cylinder that forms a hexagonal lattice [Figure 4b(ii)], which cross-links the bottlebrush PDMS matrix [Figure 4b(iii)]. Thus, an individual grain can be modeled as a fiber-reinforced composite, in which the hexagonally aligned stiff PBnMA fibers are completely bonded to the soft bottlebrush PDMS matrix. The modulus of such an aligned fiber-reinforced composite [Figure 4b(ii)] can be described by the classic Halpin—Tsai model: 33,34

$$P = \frac{1 + \zeta \eta f}{1 - \eta f} P_{\rm m} \tag{2}$$

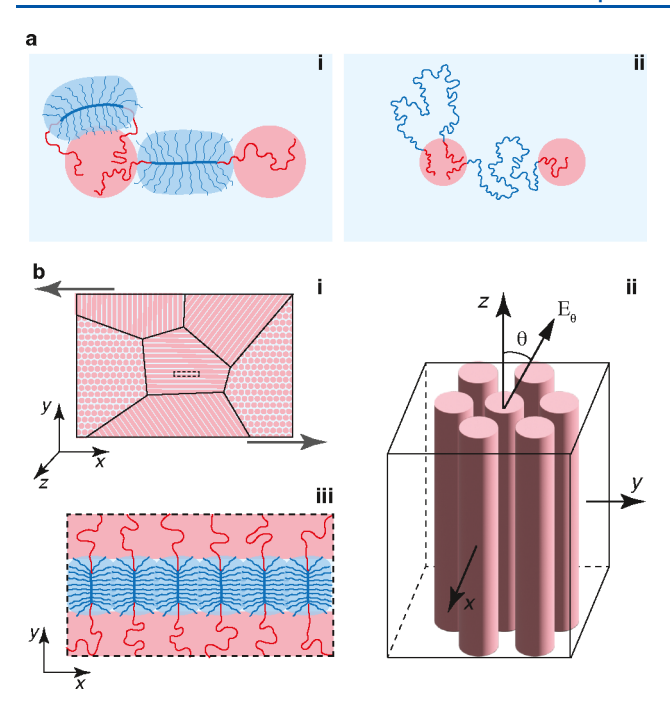


Figure 4. Molecular origin of mechanical properties of bottlebrush polymer networks. [a(i)] In sphere microstructures, an LBBL polymer can form either a loop or a bridge with negligible change in the configurational entropy because the size of the bottlebrush is comparable to that of the spherical domain. [a(ii)] By contrast, in a flexible triblock copolymer with the middle block of the same MW as that of the bottlebrush, the size of the long linear middle block is much larger than that of the spherical domain. Therefore, the formation of a loop has to overcome a free energy barrier attributed to the increase in polymer configurational entropy. (b) Fiber-reinforced composite model for LBBL polymers of cylinder morphology. (i) Reminiscent of a polycrystalline material, the bulk polymer consists of grains randomly oriented in space. (ii) In each grain, the glassy PBnMA cylinders are hexagonally packed. (iii) Moreover, each cylinder is completely bonded to the soft bottlebrush PDMS matrix. E_{θ} is Young's modulus measured at θ relative to the longitudinal axis of the cylinder. Light red: hard domains formed by end blocks; light blue: soft bottlebrush PDMS matrix.

in which f is the volume fraction of the fiber, $\eta = (P_{\rm f}/P_{\rm m}-1)/(P_{\rm f}/P_{\rm m}+\zeta)$ is a parameter largely determined by the ratio between the fiber and matrix moduli $P_{\rm f}/P_{\rm m}$, and ζ is a measure of reinforcement geometry that depends on loading conditions. For shear deformation, ζ is on the order of unity regardless of stress directions.²⁹ By contrast, for uniaxial compressive deformation or elongation along the cylinder axes, $\zeta \approx l/D$ is about the ratio between the length l and the diameter D of the cylinder. Because the diameter of a PBnMA cylinder is about 50 nm, as measured in our previous studies,²² and the typical size of a grain self-assembled by triblock copolymers is on the order of micrometers, $^{35} \zeta$ is expected to be smaller than 100. This value is much smaller than $P_{\rm f}/P_{\rm m} \sim$ 10^5 , as the modulus of PBnMA is $P_{\rm f} \sim 10^9$ Pa 36 and the modulus of soft bottlebrush PDMS is $P_{\rm m} \sim 10^4$ Pa. Therefore, the value of η is approximately 1. As a result, the modulus of the aligned fiber-reinforced composite is largely determined by the soft matrix [eq 1].

In the bulk LBBL polymer, however, not all cylinders are perfectly aligned to form a long-range ordered, anisotropic single crystal. Instead, the bulk LBBL polymer is reminiscent of a polycrystalline material with individual grains randomly

oriented in space [Figure 4b(i)]. As a result, upon shear deformation, the stress will be transmitted through grains but impinged at the grain boundary; this process effectively transforms shear into compressive deformation. Consequently, the measured macroscopic modulus G is an ensemble average of both the shear and Young's moduli of individual grains, which is expected to be dependent on the effective aspect ratio of the cylinders. Based on these considerations, we propose a modified Halpin—Tsai model for the shear modulus of a polycrystalline polymer

$$G = \frac{1 + \zeta f}{1 - f} G_{\rm m} \tag{3}$$

in which $G_{\rm m}\approx 9.4\times 10^3$ Pa is the shear modulus of a network with bottlebrush PDMS being the network strands [eq 1]. ζ is an adjustable parameter that corresponds to the effective aspect ratio of cylinders. Alternatively, ζ can be understood as the ratio between the grain size and the cylinder diameter.

The modified Halpin–Tsai model [eq 3] fits the experimental data remarkably well, as shown by the solid line in Figure 3c. Moreover, given that the diameter of cylinders is about 50 nm, ²² the fitting parameter $\zeta = 22$ suggests that the averaged grain size is on the order of 1 μ m; this value is consistent with previous findings for the grain size of triblock copolymers. ^{37–39} Collectively, our results indicate that at room temperature, LBBL triblock copolymers with cylinder morphology can be modeled as polycrystalline fiber-reinforced composites, whose shear moduli are largely determined by the matrix and increase weakly with the volume fraction of fibers.

Unlike classical fiber-reinforced composites in which the fibers are thermostable materials such as glass, in LBBL polymers, the PBnMA cylinders are plastics, whose stiffness decreases dramatically with the increase of temperature.³⁶ To explore the dependence of network mechanical properties on temperature, we monitor in real-time the viscoelasticity of LBBL polymers from -20 to 180 °C. At an oscillatory shear frequency of 1 rad/s, the storage modulus G' decreases with the increase of temperature (solid symbols in the upper panel of Figure 5a). However, G' remains larger than the loss modulus G'' for all polymers over the whole temperature range, as evidenced by the small loss factor, $\tan \delta \equiv G''/G < 1$ (the lower panel of Figure 5a). This is likely because the explored temperatures are below the melting point $T_m \approx 200$ °C of PBnMA, such that the PBnMA domains are not completely dissociated and effectively act as cross-linkers.⁶ Interestingly, the loss factor exhibits a peak near the glass-transition temperature $T_{\rm g,PBnMA}$ = 54 °C of PBnMA; yet, such a peak is seen only for polymers with relatively high-volume fractions of f > 0.3, as shown by the left arrow in the lower panel of Figure 5a. Similar behavior is observed for triblock polymers synthesized using different batches of PDMS bottlebrushes of slightly different dispersities but with the same average molecular weight (left arrow in Figure S5). This behavior suggests that the reinforcement from the glassy PBnMA fibers becomes noticeable at high-volume fractions, such that near the T_{σ} of PBnMA, the network becomes more viscous.

To further explore the contribution of PBnMA to the network stiffness, we plot the change in shear storage modulus relative to that at room temperature, $G'(T)/G'(20\,^{\circ}\text{C})$, against temperature T. Remarkably, for polymers with cylinder morphology, nearly all data points collapse to a universal curve, as shown by the symbols connected by solid lines in

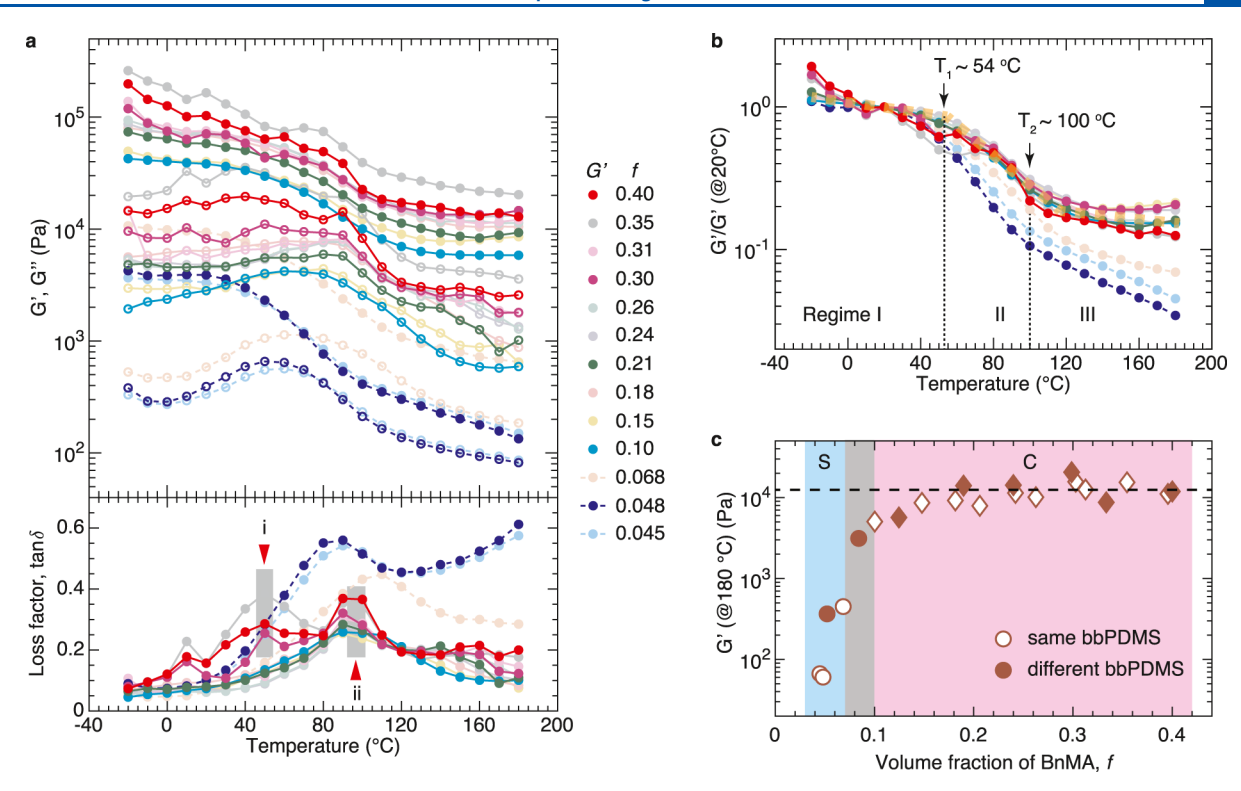


Figure 5. Effects of temperature on dynamic mechanical properties. (a) Temperature sweep and loss factor of polymers with the same bottlebrush middle block (batch 1, Table 1). Filled symbols: G' and empty symbols: G''. (b) Dependence of shear modulus normalized by that at room temperature, G'(T)/G'(20 °C), on temperature T. (c) Dependence of shear storage modulus at 180 °C on the composition f of triblock copolymers. The dashed line is the shear modulus of a bottlebrush PDMS network at temperature T = 453 K [eq 1].

Figure 5b. Moreover, the normalized shear modulus exhibits three regimes (Figure 5b). In regime I with $T < T_1 \approx T_{g,PBnMA}$ = 54 °C, G'/G'(20 °C) is nearly a constant of 1. In regime II with $T_1 < T < T_2 \approx 100$ °C, G'/G'(20 °C) decreases dramatically from 1 to ~0.2. In regime III with $T > T_2$, G'/G'(20 °C) almost does not decrease. Similar behavior is observed for triblock polymers synthesized using different batches of bottlebrush PDMS (Figure S6). Moreover, the cross-over temperature T_2 is associated with a loss tangent peak (Figure 5c). The mechanistic understanding of the cross-over temperature is beyond the scope of this study and will be the subject of future explorations. Nevertheless, these results suggest that the reinforcement to the network stiffness from the glassy PBnMA diminishes at temperatures well above $T_{\rm gPBnMA}$.

Indeed, the absolute value of the shear modulus at 180 °C is about 14 kPa, which is in excellent agreement with the theoretical prediction for the shear modulus of a bottlebrush PDMS network at temperature $T = 453 \text{ K} \left[\text{eq 1}\right]$, as indicated by the horizontal dashed line in Figure 5c. Note that this agreement suggests two features unique to LBBL polymers with cylinder morphology. First, the fraction of loops is nearly zero; this is consistent with existing findings that in triblock copolymers, a semiflexible middle block easily promotes the formation of bridges to >95% at relatively high-end block volume fractions. 40 Second, even at high temperatures above the T_{σ} of the glassy domains, the linear blocks are too long to be completely pulled out from the glassy domains, such that nearly all bottlebrush polymers remain elastically effective by bridging two neighboring glassy domains. By contrast, for LBBL polymers with sphere morphology of low $f \approx 0.05$, the network shear modulus continues to decrease rather than

being a constant (dashed lines in the upper panel of Figure Sa,b). This is likely because at high temperatures, the end blocks are relatively short and can be pulled out from the spherical domains; this process transforms elastically effective bridges to elastically ineffective dangling bbPDMS polymers, resulting in the decrease of the network shear modulus. Taken together, these results suggest that at temperatures well above the $T_{\rm g}$ of glassy domains, the network shear modulus is largely determined by the elastomeric bottlebrush matrix.

3. CONCLUSIONS

In summary, we have systematically investigated the effects of composition on the dynamic mechanical properties of LBBL triblock copolymers. We find that the polymer shear modulus G exhibits two regimes depending on the volume fraction f of the end blocks or network morphology. (i) At small volume fractions or sphere morphology, the network shear modulus is nearly a constant. Yet, because of a large fraction of loops, the absolute value of G is about 40% of the soft bottlebrush matrix, $G_m \approx k_{\rm B} T \rho / M_{\rm bb}$ [eq 1]. (ii) At relatively high-volume fractions or cylinder morphology, G increases slowly with the composition but remains nearly 4 orders of magnitude lower than that of hard, glassy cylinders. To explain the experimental observation, we propose that the polymer consists of randomly oriented grains, each of which can be modeled as a fiberreinforcement composite. The macroscopic shear modulus of such a polycrystalline material can be described by a modified Halpin–Tsai model, $G = G_{\rm m}(1 + \zeta f)/(1 - f)$, in which ζ is an adjustable parameter that describes the grain size relative to the fiber diameter [eq 3]. At high temperatures well above the T_{σ} of the glassy domains, the reinforcement to the network

modulus from the glassy fibers diminishes, such that the shear modulus becomes a constant of the matrix stiffness.

We note a few outstanding questions regarding the mechanical properties of self-assembled BPNs. For example, what is the molecular origin of the observed exponential increase in network stiffness as the network transitions from sphere to cylinder morphology? What is the relation between the stiffness of BPNs and the composition of lamellar morphology? Finally, how does the flexibility of the bottlebrush affect the mechanical properties? These questions are beyond the scope of this paper and will be the subject of future explorations.

Nevertheless, our results provide a new approach to controlling the stiffness of bottlebrush polymer networks. Unlike existing chemically cross-linked bottlebrush polymer networks, whose stiffness is controlled by the concentration of cross-linkers, for the self-assembled bottlebrush networks, the stiffness can be tuned by solely changing the composition or the network morphology. Moreover, the self-assembled BPNs are reprocessable using solvents; this would enable the polymers as a new class of sustainable materials and a class of soft inks for additive manufacturing.^{6,41} Furthermore, the developed polymeric materials have controllable stiffness from ~4 to ~100 kPa, covering the range of soft biological tissues and hydrogels.¹⁰ Because the bottlebrush polymer networks are purely elastic, they may be used as substrates to decouple the effects of elasticity and material relaxation on the behavior of cells. 42,43 Thus, our results not only help establish the molecule-structure-property relation of self-assembled bottlebrush polymer networks but also provide a new class of solvent-free and reprocessable polymeric materials with a wide range of controllable stiffnesses.

4. EXPERIMENTAL SECTION

- **4.1. Materials.** MCR-M17, monomethacryloxypropyl-terminated polydimethylsiloxane, with an average molar mass of 5000 g/mol, was purchased from Gelest and purified using basic aluminum oxide columns to remove inhibitors before use. Benzyl methacrylate (96%) was purchased from Sigma-Aldrich and purified using basic aluminum oxide columns to remove inhibitors before use. Copper(II) chloride (CuCl₂, 99.999%), tris[2-(dimethylamino)ethyl]amine(Me₀TREN), ethylene bis(2-bromoisobutyrate) (2f-BiB, 97%), tin(II) 2-ethylhexanoate (Sn(EH)₂, 92.5−100%), anisole (≥99.7%), and p-xylene (≥99.7%) were purchased from Sigma-Aldrich and used as received. Methanol (Certified ACS), diethyl ether (Certified ACS), dimethylformamide (DMF, Certified ACS), tetrahydrofuran (THF, Certified ACS), and THF (HPLC) were purchased from Fisher and used as received.
- **4.2. Polymer Synthesis and Characterization.** The synthesis and characterization of all LBBL polymers are detailed in our previous publication, ²² except for batch 5 (Table 1). For batch 5, the gel permeation chromatography traces are shown in Figure S7. The volume fraction of PBnMA is determined based on the ¹H NMR of purified triblock copolymers (see Supporting Information ¹H NMR Spectra) using a method documented in a previous publication. ⁵
- **4.3. Rheometry.** Rheological measurements are performed using a stress-controlled rheometer (Anton Paar MCR 302) equipped with a plate—plate geometry of 8 mm in diameter. For thermal annealing, we use a slow temperature ramping rate of 1 °C/minute, increase the temperature from 60 to 180 °C, and hold it at 180 °C for 30 min. Upon cooling, we wait for 20 min at each temperature point before collecting data; this ensures that the self-assembled microstructure is in equilibrium at each temperature point. During these processes, the oscillatory shear strain is fixed at 0.5%, and the shear frequency is 1 rad/s. For frequency sweep, the measurement at each temperature point is performed after waiting for 20 min with the oscillatory shear

strain at 0.5% while varying the shear frequency from 0.1 rad/s to 100 rad/s. For temperature sweep, the storage and loss moduli after waiting for 20 min at each temperature point are used. The temperature points range from -20 to $180\,^{\circ}\mathrm{C}$ with an interval of $10\,^{\circ}\mathrm{C}$. For strain sweep, we restore the temperature to $20\,^{\circ}\mathrm{C}$ with a ramping rate of $1\,^{\circ}\mathrm{C/min}$, wait for 20 min, and fix the frequency at 1 rad/s while increasing the shear strain from 0.1 to 1000%.

ASSOCIATED CONTENT

Supporting Information

The Supporting Information is available free of charge at https://pubs.acs.org/doi/10.1021/acs.macromol.2c01204.

Thermal annealing, frequency sweep, strain sweep, yield strain, temperature seep of self-assembled bottlebrush polymer networks, gel permeation chromatography traces, and ¹H NMR spectra for polymers in batch 5 (PDF)

AUTHOR INFORMATION

Corresponding Author

Li-Heng Cai — Soft Biomatter Laboratory, Department of Materials Science and Engineering, University of Virginia, Charlottesville, Virginia 22904, United States; Department of Chemical Engineering and Department of Biomedical Engineering, University of Virginia, Charlottesville, Virginia 22904, United States; Orcid.org/0000-0002-6806-0566; Email: liheng.cai@virginia.edu

Author

Shifeng Nian — Soft Biomatter Laboratory, Department of Materials Science and Engineering, University of Virginia, Charlottesville, Virginia 22904, United States; orcid.org/0000-0002-2243-6329

Complete contact information is available at: https://pubs.acs.org/10.1021/acs.macromol.2c01204

Notes

The authors declare no competing financial interest.

ACKNOWLEDGMENTS

We thank Shiwang Cheng (Michigan State University), Timothy Lodge (University of Minnesota), and Edwin Thomas (Texas A&M) for enlightening discussions. L.H.C. acknowledges the support from NSF (CAREER DMR-1944625) and ACS Petroleum Research Fund (PRF) (6132047-DNI).

REFERENCES

- (1) Cai, L.-H.; Kodger, T. E.; Guerra, R. E.; Pegoraro, A. F.; Rubinstein, M.; Weitz, D. A. Soft Poly(Dimethylsiloxane) Elastomers from Architecture-Driven Entanglement Free Design. *Adv. Mater.* **2015**, *27*, 5132–5140.
- (2) Paturej, J. J.; Sheiko, S. S.; Panyukov, S.; Rubinstein, M. Molecular Structure of Bottlebrush Polymers in Melts. *Sci. Adv.* **2016**, 2, No. e1601478.
- (3) Daniel, W. F. M. M.; Burdyńska, J.; Vatankhah-Varnoosfaderani, M.; Matyjaszewski, K.; Paturej, J.; Rubinstein, M.; Dobrynin, A. V.; Sheiko, S. S. Solvent-Free, Supersoft and Superelastic Bottlebrush Melts and Networks. *Nat. Mater.* **2016**, *15*, 183–189.
- (4) Vatankhah-Varnosfaderani, M.; Keith, A. N.; Cong, Y.; Liang, H.; Rosenthal, M.; Sztucki, M.; Clair, C.; Magonov, S.; Ivanov, D. A.; Dobrynin, A. V.; et al. Chameleon-like Elastomers with Molecularly Encoded Strain-Adaptive Stiffening and Coloration. *Science* **2018**, 359, 1509–1513.

- (5) Nian, S.; Lian, H.; Gong, Z.; Zhernenkov, M.; Qin, J.; Cai, L.-H. Molecular Architecture Directs Linear—bottlebrush—linear Triblock Copolymers to Self-Assemble to Soft Reprocessable Elastomers. *ACS Macro Lett.* **2019**, *8*, 1528—1534.
- (6) Nian, S.; Zhu, J.; Zhang, H.; Gong, Z.; Freychet, G.; Zhernenkov, M.; Xu, B.; Cai, L. H. Three-Dimensional Printable, Extremely Soft, Stretchable, and Reversible Elastomers from Molecular Architecture-Directed Assembly. *Chem. Mater.* **2021**, 33, 2436–2445.
- (7) Gong, J. P.; Katsuyama, Y.; Kurokawa, T.; Osada, Y. Double-Network Hydrogels with Extremely High Mechanical Strength. *Adv. Mater.* **2003**, *15*, 1155.
- (8) Sun, J.-Y.; Zhao, X.; Illeperuma, W. R. K. K.; Chaudhuri, O.; Oh, K. H.; Mooney, D. J.; Vlassak, J. J.; Suo, Z. Highly Stretchable and Tough Hydrogels. *Nature* **2012**, *489*, 133–136.
- (9) Creton, C. Anniversary Perspective: Networks and Gels: Soft but Dynamic and Tough. *Macromolecules* **2017**, *50*, 8297–8316.
- (10) Levental, I.; Georges, P. C.; Janmey, P. A. Soft Biological Materials and Their Impact on Cell Function. *Soft Matter* **2007**, *3*, 299–306.
- (11) Reynolds, V. G.; Mukherjee, S.; Xie, R.; Levi, A. E.; Atassi, A.; Uchiyama, T.; Wang, H.; Chabinyc, M. L.; Bates, C. M. Super-Soft Solvent-Free Bottlebrush Elastomers for Touch Sensing. *Mater Horizons* **2020**, *7*, 181–187.
- (12) Vatankhah-Varnoosfaderani, M.; Daniel, W. F. M. M.; Zhushma, A. P.; Li, Q.; Morgan, B. J.; Matyjaszewski, K.; Armstrong, D. P.; Spontak, R. J.; Dobrynin, A. V.; Sheiko, S. S. Bottlebrush Elastomers: A New Platform for Freestanding Electroactuation. *Adv. Mater.* **2017**, *29*, 1604209.
- (13) Xu, P.; Wang, S.; Lin, A.; Min, H.-K.; Zhou, Z.; Huang, X.; Tran, H.; Liu, X. Conductive SWCNT/PDMS Bottlebrush Elastomers for Ultrasoft Electronics, **2022**. DOI: 10.26434/chemrxiv-2022-n6mp5.
- (14) Cushman, K.; Keith, A.; Tanaka, J.; Sheiko, S. S.; You, W. Investigating the Stress-Strain Behavior in Ring-Opening Metathesis Polymerization-Based Brush Elastomers. *Macromolecules* **2021**, *54*, 8365–8371.
- (15) Cai, L.-H. Molecular Understanding for Large Deformations of Soft Bottlebrush Polymer Networks. *Soft Matter* **2020**, *16*, 6259–6264.
- (16) Mukherjee, S.; Xie, R.; Reynolds, V. G.; Uchiyama, T.; Levi, A. E.; Valois, E.; Wang, H.; Chabinyc, M. L.; Bates, C. M. Universal Approach to Photo-Cross-link Bottlebrush Polymers. *Macromolecules* **2020**, 53, 1090–1097.
- (17) Arrington, K. J.; Radzinski, S. C.; Drummey, K. J.; Long, T. E.; Matson, J. B. Reversibly Cross-Linkable Bottlebrush Polymers as Pressure-Sensitive Adhesives. *ACS Appl. Mater. Interfaces* **2018**, *10*, 26662–26668.
- (18) Sarapas, J. M.; Chan, E. P.; Rettner, E. M.; Beers, K. L. Compressing and Swelling to Study the Structure of Extremely Soft Bottlebrush Networks Prepared by ROMP. *Macromolecules* **2018**, *51*, 2359–2366.
- (19) Dashtimoghadam, E.; Fahimipour, F.; Keith, A. N.; Vashahi, F.; Popryadukhin, P.; Vatankhah-Varnosfaderani, M.; Sheiko, S. S. Injectable Non-Leaching Tissue-Mimetic Bottlebrush Elastomers as an Advanced Platform for Reconstructive Surgery. *Nat. Commun.* **2021**, *12*, 3961.
- (20) Self, J. L.; Sample, C. S.; Levi, A. E.; Li, K.; Xie, R.; de Alaniz, J.; Bates, C. M. Dynamic Bottlebrush Polymer Networks: Self-Healing in Super-Soft Materials. *J. Am. Chem. Soc.* **2020**, *142*, 7567.
- (21) Choi, C.; Self, J. L.; Okayama, Y.; Levi, A. E.; Gerst, M.; Speros, J. C.; Hawker, C. J.; Read de Alaniz, J.; Bates, C. M. Light-Mediated Synthesis and Reprocessing of Dynamic Bottlebrush Elastomers under Ambient Conditions. J. Am. Chem. Soc. 2021, 143, 9866–9871.
- (22) Nian, S.; Fan, Z.; Freychet, G.; Zhernenkov, M.; Redemann, S.; Cai, L. H. Self-Assembly of Flexible Linear-Semiflexible Bottlebrush-Flexible Linear Triblock Copolymers. *Macromolecules* **2021**, *54*, 9361–9371.

- (23) Segalman, R. A. Patterning with Block Copolymer Thin Films. *Mater. Sci. Eng.*, R **2005**, 48, 191–226.
- (24) Hutchinson, J. M. Physical Aging of Polymers. *Prog. Polym. Sci.* **1995**, *20*, 703–760.
- (25) Cangialosi, D.; Alegría, A.; Colmenero, J. Effect of Nanostructure on the Thermal Glass Transition and Physical Aging in Polymer Materials. *Prog. Polym. Sci.* **2016**, 54-55, 128–147.
- (26) Matsen, M. W. Equilibrium Behavior of Symmetric ABA Triblock Copolymer Melts. J. Chem. Phys. 2000, 113, 5539-5544.
- (27) Rubinstein, M.; Colby, R. H. Polymer Physics; Oxford University Press: Oxford, U.K., 2003.
- (28) Allan, P.; Arridge, R. G. C.; Ehtaiatkar, F.; Folkes, M. J. The Mechanical Properties of an Oriented Lamella Stock Formed from an S-B-S Block Copolymer. *J. Phys. D: Appl. Phys.* **1991**, 24, 1381–1390.
- (29) Arridge, R. G. C.; Folkes, M. J. The Mechanical Properties of a "single Crystal" of SBS Copolymer a Novel Composite Material. *J. Phys. D: Appl. Phys.* **1972**, *5*, 344–358.
- (30) Dair, B. J.; Honeker, C. C.; Alward, D. B.; Avgeropoulos, A.; Hadjichristidis, N.; Fetters, L. J.; Capel, M.; Thomas, E. L. Mechanical Properties and Deformation Behavior of the Double Gyroid Phase in Unoriented Thermoplastic Elastomers. *Macromolecules* 1999, 32, 8145–8152.
- (31) Bates, F. S.; Fredrickson, G. H. Block Copolymers-Designer Soft Materials. *Phys Today* **1999**, *52*, 32–38.
- (32) Honeker, C. C.; Thomas, E. L. Impact of Morphological Orientation in Determining Mechanical Properties in Triblock Copolymer Systems. *Chem. Mater.* **1996**, *8*, 1702–1714.
- (33) Tsai, S. W.; Wu, E. M. A General Theory of Strength for Anisotropic Materials. *J Compos Mater* 1971, 5, 58–80.
- (34) Halpin, J. C.; Louis, S. T.; Kardos, J. L.; Halpin, C.; Louis, S. T.; Kardos, L. The Halipin-Tsai Equaations: A Review. *Polym. Eng. Sci.* 1976, 16, 344–352.
- (35) Balsara, N. P.; Dai, H. J.; Watanabe, H.; Sato, T.; Osaki, K. Influence of Defect Density on the Rheology of Ordered Block Copolymers. *Macromolecules* **1996**, 29, 3507–3510.
- (36) Calleja, R. D.; Gargallo, L.; Radic, D. Dynamic Mechanical Behaviour of Poly(Benzyl Methacrylate) and Poly(Cyclohexylmethyl Methacrylate). *Polymer* 1993, 34, 4247–4251.
- (37) Jinnai, H.; Yasuda, K.; Nishi, T. Three-Dimensional Observations of Grain Boundary Morphologies in a Cylinder-Forming Block Copolymer. *Macromol. Symp.* **2006**, 245–246, 170–174.
- (38) Ohnogi, H.; Isshiki, T.; Sasaki, S.; Sakurai, S. Intriguing Transmission Electron Microscopy Images Observed for Perpendicularly Oriented Cylindrical Microdomains of Block Copolymers. *Nanoscale* **2014**, *6*, 10817–10823.
- (39) Ohnogi, H.; Sasaki, S.; Sakurai, S. Evaluation of Grain Size by Small-Angle X-Ray Scattering for a Block Copolymer Film in Which Cylindrical Microdomains Are Perpendicularly Oriented. *Macromol. Symp.* **2016**, 366, 35–41.
- (40) Shah, M.; Ganesan, V. Chain Bridging in a Model of Semicrystalline Multiblock Copolymers. *J. Chem. Phys.* **2009**, *130*, 3072339.
- (41) Zhu, J.; He, Y.; Kong, L.; He, Z.; Kang, K. Y.; Grady, S. P.; Nguyen, L. Q.; Chen, D.; Wang, Y.; Oberholzer, J.; et al. Digital Assembly of Spherical Viscoelastic Bio-Ink Particles. *Adv. Funct. Mater.* **2022**, 32, 2109004.
- (42) Chaudhuri, O.; Gu, L.; Klumpers, D.; Darnell, M.; Bencherif, S. A.; Weaver, J. C.; Huebsch, N.; Lee, H. P.; Lippens, E.; Duda, G. N.; et al. Hydrogels with Tunable Stress Relaxation Regulate Stem Cell Fate and Activity. *Nat. Mater.* **2016**, *15*, 326–334.
- (43) Chaudhuri, O.; Cooper-White, J.; Janmey, P. A.; Mooney, D. J.; Shenoy, V. B. Effects of Extracellular Matrix Viscoelasticity on Cellular Behaviour. *Nature* **2020**, *584*, 535–546.